Synthesis and Hemocompatibilities of New Segmented Polyurethanes and Poly(urethane urea)s with Poly(butadiene) and Phosphatidylcholine Analogues in the Main Chains and Long-Chain Alkyl Groups in the Side Chains

Yu-Jun Li,[†,§] Naotoshi Nakamura,[†,⊥] Yan-Feng Wang,[†] Makoto Kodama,[‡] and Tadao Nakaya*[,†]

Department of Bioapplied Chemistry, Faculty of Engineering, Osaka City University, 3-3-138 Sugimoto, Sumiyoshi-ku, Osaka 558, Japan, and Bionic Design Group, National Institute for Advanced Interdisciplinary Research, 1-1-4 Higashi, Tsukuba, Ibaraki 305, Japan

Received December 4, 1996[⊗]

Three new phospholipid diols, bis[2-(2-hydroxyethyldimethylammonio)ethyl]diethylene octadecylamine diphosphate (BDODP), bis[2-(2-hydroxyethyldimethylammonio)ethyl]diethylene hexadecylamine diphosphate (BDHDP), and bis[2-(2-hydroxyethyldimethylammonio)ethyl]-diethylene dodecylamine diphosphate (BDDDP), together with 1,4-butanediol (BD) or ethylenediamine (ED) as chain extender were further incorporated into the prepolymer of poly(butadiene) glycol (PBD) and 4,4′-methylenediphenyl diisocyanate (MDI). The bulk and surface characteristics of the resulting phospholipid segmented polyurethanes (SPUs) and segmented poly(urethane urea)s (SPUUs) were investigated by infrared (IR), gel permeation chromatography (GPC), attenuated total reflectance Fourier transform infrared spectroscopy (ATR-FTIR), electron spectroscopy for chemical analysis (ESCA), and contact angle measurements. The mechanical properties were investigated by dynamic viscoelasticity. The hemocompatibilities of the new polymers were evaluated by platelet-rich plasma (PRP) contact studies and viewed by scanning electron microscopy (SEM) using medical BioSpan as a reference. It was found that the new polymers possessed relatively hydrophobic surfaces revealed by contact angle measurements. Moreover, the new materials have good surfaces in terms of platelet adhesion and that the morphology of adhered platelets undergoes a relatively low degree of variation.

Introduction

Heart valves and other synthetic prosthetic devices in contact with living tissue must be compatible with their biological host. To obtain polymers with biocompatible surfaces, a number of surface modification approaches have been taken. One approach has involved grafting an alkyl side chain on the poly(ether urethane) backbone, where the modified polymers show a high affinity for albumin adsorption and low platelet reactivity.[1−3] Another approach has involved introducing long alkyl side chains on to a polyurethane, which has shown to reduce platelet deposition and enhance in vitro albumin adsorption.[4−8] More interest and an important approach is that of incorporating phospholipids onto polymers.[9] To obtain biocompatible polymers in artificial organs, in 1986 we successfully synthesized phospholipid-like diols and polyurethanes.[10] Recently we have developed some new polyurethanes bearing phosphatidylcholine analogues in the main chains[11,12] and side chains.[13−16] Some other phospholipid biomaterials have been made either by introducing phosphatidylcholine derivatives as plasticizers into polymers such

† Osaka City University.
‡ National Institute for Advanced Interdisciplinary Research.
§ Present address: Procter & Gamble Far East, Inc. 17, Koyo-cho Naka 1-chome, Higashinada-ku, Kobe 658, Japan.
⊥ Present address: Kansai Polymer Research Laboratory, Toyo Ink MFG. Co., LTD, Fukushima-ku, Osaka 553, Japan.
* To whom correspondence should be addressed at the Osaka City University. E-mail: nakaya@bioa.eng.osaka-cu.ac.jp.
⊗ Abstract published in *Advance ACS Abstracts,* June 1, 1997.

(1) Munro, M. S.; Eberhart, R. C.; Maki, N. J.; Brink, B. E.; Fry, W. J. *ASAIO J.* **1983**, *6*, 65.
(2) Grasel, T. G.; Pierce, J. A.; Cooper, S. L. *J. Biomed. Mater. Res.* **1987**, *21*, 815.
(3) Pitt, W. G.; Grasel, T. G.; Cooper, S. L. *Biomaterials* **1988**, *9*, 36.
(4) Eberhart, R. C.; Munro, M. S.; Williams, G. B.; Kulcarni, P. V.; Shannon, W. A.; Brink, B. E.; Fly, W. J. *Artif. Organs* **1987**, *11*, 375.
(5) Rahman, R.; Ratner, B. D. *J. Polym. Sci., Part A: Polym. Chem.* **1989**, *27*, 2673.
(6) Strizinar, I.; Sefton, M. *J. Biomed. Mater. Res.* **1992**, *26*, 577.
(7) Marconi, W.; Martinelli, A.; Piozzi, A.; Zane, D. *Macromol. Chem. Phys.* **1994**, *195*, 875.
(8) Marconi, W.; Galloppa, A.; Martinelli, A.; Piozzi, A. *Biomaterials* **1995**, *16*, 449.
(9) Nakaya, T.; Li, Y.-J. Polymeric Phospholipid Analogues. In: *Encyclopedia of Polymer Science and Technology*; Cheremisinoff, N. P., Ed.; Marcel Dekker Publishers: New York, in press.
(10) Nakaya, T.; Yamada, M.; Imoto, M. Jpn. Patent 61-207395, 1986 (*Chem. Abstr.* **1987**, *106*, 177059).
(11) Yamada, M.; Li, Y.-J.; Nakaya, T. *Macromol., Rapid Commun.* **1995**, *16*, 25.
(12) Li, Y.-J.; Zhang, Z.; Kodama, M.; Nakaya, T. *J. Biomater. Appl.*, in press.
(13) Yamada, M.; Li, Y.-J.; Nakaya, T. *J. Macromol. Sci.-Pure Appl. Chem.* **1995**, *A32*, 1235.
(14) Li, Y.-J.; Shibata, Y.; Nakaya, T. *Macromol., Rapid Commun.* **1995**, *16*, 253.
(15) Li, Y.-J.; Matthews, K. H.; Kodama, M.; Nakaya, T. *Macromol. Chem. Phys.* **1995**, *196*, 3143.
(16) Li, Y.-J.; Bahulekar, R.; Chen, T.-M.; Wang, Y.-F.; Kodama, M.; Nakaya, T. *Macromol. Chem. Phys.* **1996**, *197*, 2827.

S0897-4756(96)00615-1 CCC: $14.00

as poly(vinyl chloride) (PVC) and polyurethane[17] or by copolymerizing phosphatidylcholine monomers into the polymer backbone of polyurethanes and polyesters.[18,19] The phosphatidylcholine polar headgroups can be attached on many surfaces by a number of different ways, and large improvements in hemocompatibility have been observed.[20−23]

On the other hand, many approaches to construct polyurethanes with biostability have also been performed. The inventory of currently used biomaterials for these devices includes the so-called segmented polyurethanes (SPUs). However, the SPUs most frequently used today in biomedical applications are poly(ether urethane)s and subject to significant degradation under certain conditions of mechanical or chemical action of implanted devices.[24−27] One of the major causes of degradation is oxidation of the polyether chain.

To develop polyurethane biomaterials that are more stable in vivo, it may be desirable to prepare SPUs without ether-containing polydiols. Cooper and coworkers[28] used several nonether polydiols such as poly(butadiene), hydrogenated poly(butadiene), and poly(dimethylsiloxane) chain segments to synthesize SPUs. It was concluded that polyurethanes with aliphatic hydrocarbon-based polyol components are stable against oxidative degradation. Moreover, a recent investigation shows that SPUs that do not contain the ether linkage in the polyol component do not inhibit metabolic cooperation and might be less prone to cause tumor formation than polyether-based polyurethane.[29]

We have recently made a new type of SPU that shows excellent mechanical strength as well as significant blood compatibility.[30−34] As with other SPUs, the novel polymers have both hard and soft segments. But we avoided using the ether type molecules previously used in making the soft segment and introduced different phospholipids into the polyurethanes. Moreover, phospholipid poly(urethane urea)s with non-ether polydiol soft segments and amphiphilic microphase-separated domain structures are also synthesized in this laboratory.[35] Our previous results suggest that incorporating phospholipids and long-chain alkyl groups into polymer side chains may improve the hemocompatibilities and introducing suitable non-ether soft segments into the polymer main chain may improve the mechanical properties.

In a recent study of this series, we have designed and reported another new type of comblike phospholipid diol and polyurethane, with long alkyl groups remaining in the side chains but changing the phosphatidylcholine analogues in the polymer backbone.[36,37] Investigating the hemocompatibility of this new type of phospholipid polymer has not been carefully studied yet. To this end, the main aim of this study is to synthesize new polymers with hydrophilic phosphatidylcholine analogues in the main chains and hydrophobic long alkyl groups in the side chains and further investigate their hemocompatibility. From the biostability point of view, we also chose the non-ether poly(butadiene) glycol as the soft segment. Bulk characterization of the polymers included infrared (IR) and gel permeation chromatography (GPC) measurements. The mechanical property investigation included dynamic viscoelasticity measurement. Surface characterization was performed by contact angle measurements, attenuated total reflectance Fourier transform infrared spectroscopy (ATR-FTIR), and electron spectroscopy for chemical analysis (ESCA). The hemocompatibility of the polymers was evaluated by describing the platelet state and shape variation for the attached platelets.

Experimental Section

General Method. To obtain a solution suitable for casting on test surfaces, after briefly drying under vacuum to remove residual methanol, the resulting polymers were dissolved in mixed *N,N*-dimethylacetamide (DMAc) and tetrahydrofuran (THF, volume ratio 1/1) solution by ultrasonic generator. The obtained polymer solutions were defoamed by evaporator in a desiccator and then cast onto a glass plate to create films for bulk property testing or surface property experiments. In casting procedure, the casting films were first dried in an oven at 70 °C under flowing nitrogen for at least 48 h to remove most of the solvents. The final drying stage involved drying the sheet in a vacuum oven at 70 °C for at least 48 h to remove residual solvents. The IR spectral analyses of the polymers were taken on cast films and using a Jasco A 202 spectrometer. GPC measurements were performed on a HLC802UR GPC instrument with G4000H8 + G2000H8 columns; the samples were dissolved in mixed solvent of THF and DMAc (volume ratio 1/1) and using narrow molecular weight polystyrene as standards. The temperature dependence of the dynamic viscoelasticity of the samples was obtained using a microprocessor-controlled Rheovibron DDV-01FP under a dry nitrogen purge. Two typical samples (454 μm thick, 2 mm wide, 30 mm long for SPU-**12**, and 105 μm thick, 2 mm wide, 30 mm long for SPUU-**12**) were cooled to −150 °C, and data subsequently taken at a test frequency of 11 Hz and heating rate of 3 °C min^{-1}. ATR-FTIR was performed on the surfaces of the cast films. The spectrum was collected at 4 cm^{-1} resolution using a Jasco Micro FT/IR-200 microsampling spectrometer over 50 scans. The sampling area was 25 μm^2, coupled with an ATR accessory and 45° KRS-5 crystal. ESCA spectra were obtained on a Shimadzu ESCA 750 spectrometer using Mg Kα radia-

(17) Valencia, G. P. European Patent 247114, 1985.
(18) Chapman, D.; Valencia, G. P. European Patent 199790, 1984.
(19) Durrani, A. A. European Patent 275293, 1986.
(20) Durrani, A. A.; Hayward, J. A.; Chapman, D. *Biomaterials* **1986**, *7*, 121.
(21) Letourneur, D.; Douzon, C.; Jozefowicz, M. *J. Polym. Sci., Part A: Polym. Chem.* **1991**, *29*, 1367.
(22) Ishihara, K.; Ziats, N. P.; Tierney, B. P.; Nakabayashi, N.; Anderson, J. M. *J. Biomed. Mater. Res.* **1991**, *25*, 1397.
(23) Ishihara, K.; Oshida, H.; Endo, Y.; Ueda, T.; Watanabe, A.; Nakabayashi, N. *J. Biomed. Mater. Res.* **1992**, *26*, 1543.
(24) Coury, A. J.; Stokes, K. B.; Cahalan, P. T.; Slaikeu, P. C. *Life Support Syst.* **1987**, *5*, 25.
(25) Coury, A. J.; Slaikeu, P. C.; Cahalan, P. T.; Stokes, K. B.; Hobot, C. M. *J. Biomater. Appl.* **1988**, *3*, 130.
(26) Takahara, A.; Takamori, K.; Kajiyama, T. *Artificial Heart 2*; Akutsu, T., Ed.; Springer-Verlag: Tokyo, 1988; p 19.
(27) Takahara, A.; Hergenrother, R. W.; Coury, A. J.; Cooper, S. L. *J. Biomed. Mater. Res.* **1991**, *25*, 341.
(28) Takahara, A.; Okkema, A. Z.; Cooper, S. L.; Coury, A. J. *Biomaterials* **1991**, *12*, 324.
(29) Tsuchiya, T.; Takahara, A.; Cooper, S. L.; Nakamura, A. *J. Biomed. Mater. Res.* **1995**, *29*, 835.
(30) Li, Y.-J.; Yokawa, T.; Matthews, K. H.; Chen, T.-M.; Wang, Y. F.; Kodama, M.; Nakaya, T. *Biomaterials* **1996**, *17*, 2179.
(31) Li, Y.-J.; Matthews, K. H.; Chen, T.-M.; Wang, Y. F.; Kodama, M.; Nakaya, T. *Chem. Mater.* **1996**, *8*, 1441.
(32) Li, Y.-J.; Bahulekar, R.; Wang, Y.-F.; Chen, T.-M.; Kitamura, M.; Kodama, M.; Nakaya, T. *J. Biomater. Sci. Polym. Ed.* **1996**, *7*, 893.
(33) Li, Y.-J.; Matthews, K. H.; Wang, Y. F.; Chen, T.-M.; Kodama, M.; Nakaya, T. *J. Appl. Polym. Sci.* **1996**, *62*, 687.
(34) Li, Y.-J.; Nakaya, T. Presented at International Symposium of Polycondensation '96, in Paris, September 1996; *Macromol. Symp.* submitted.
(35) Chen, T.-M.; Wang, Y. F.; Li, Y.-J.; Kitamura, M.; Nakaya, T. *Macromol. Chem. Phys.* **1996**, *197*, 1587.
(36) Li, Y.-J.; Nakamura, N; Chen, T.-M.; Wang, Y.-F.; Kitamura, M.; Nakaya, T. *Macromol., Rapid Commun.* **1996**, *17*, 737.
(37) Korematsu, A; Li, Y.-J.; Nakaya, T. *Polym. Bull.* **1997**, *38*, 133.

Table 1. Synthesis and Bulk Property Characterization of the Phospholipid SPUs and SPUUs[a]

	second step[b]				third step						GPC data[c]		
polymers	BDODP/DMAc (g/mL)	BDHDP/DMAc (g/mL)	BDDDP/DMAc (g/mL)	reaction time at 95 °C (h)	BD/DMAc (g/mL)	ED/DMAc (g/mL)	reaction time at 100 °C (h)	precipitating solvent	yield (%)	hard segment (%)	$M_w \times 10^4$	$M_n \times 10^4$	(M_w/M_n)
SPU-**18**	0.988/15			3	0.119/15		1	methanol	85	31.5	5.6	3.0	1.9
SPU-**16**		0.951/15		3	0.119/15		1	methanol	82	31.1	5.4	3.4	1.6
SPU-**12**			0.876/15	3	0.119/15		1	methanol	80	30.4	5.9	3.5	1.7
SPUU-**18**	0.988/15			3		0.079/15	1	methanol	86	31.1	7.6	4.2	1.8
SPUU-**16**		0.951/15		3		0.079/15	1	methanol	84	30.7	7.5	5.0	1.5
SPUU-**12**			0.876/15	3		0.079/15	1	methanol	82	30.0	7.2	4.5	1.6

[a] SPU, segmented polyurethane; SPUU, segmented poly(urethane urea); PBD, poly(butadiene) glycol; MDI, 4,4′-methylenediphenyl diisocyanate; BDODP, bis[2-(2-hydroxyethyldimethylammonio)ethyl]diethylene octadecylamine diphosphate; BDHDP, bis[2-(2-hydroxyethyldimethylammonio)ethyl]diethylene hexadecylamine diphosphate; BDDDP, bis[2-(2-hydroxyethyldimethylammonio)ethyl]diethylene dodecylamine diphosphate; BD, 1,4-butanediol; ED, ethylenediamine; DMAc, *N*,*N*-dimethylacetamide. [b] First step was performed by reacting 5.0 g of PBD and 1.101 g of MDI in 20 mL of DMAc at 75 °C for 1 h. [c] Determined by GPC using polystyrene as standards.

tion. The cast films after peeling from the glass were mounted on the specimen holder. The typical operating conditions included maintaining the X-ray gun at 8 kV and 30 mA, reducing the pressure in the sample chamber to about 3×10^{-5} Pa. The takeoff angle of the photoelectron was 60°. The repeat time was one time for carbon and oxygen and five times for nitrogen and phosphorus, respectively. In addition to taking survey scans (0−1000 eV) with a view to determining the elemental composition of the various surfaces, elemental compositions were also determined on the basis of peak areas from the C_{1s}, N_{1s}, O_{1s}, and P_{2p} orbitals. Peak areas were calculated using the standard Shimadzu ESPAC 100 software. The binding energy was referenced by setting the C_{1s} hydrocarbon peak to 285 eV.

Contact Angle Measurements. Contact angles between the resulting six polymer cast film samples and pure water were measured by using a Model CA-A contact-angle meter (Kyowa Inter Face Science Co., Ltd., Japan). The values quoted are the average of 12 measurements of each sample taken at 3 min contact of the water droplet on the air-exposed side. The procedure of hemocompatibility evaluation for blood platelet adhesion and shape variation was the same as that described previously.[15] In briefly, the six cast films were washed with saline and incubated at 37 °C for 1 h with freshly prepared, platelet-rich plasma (PRP) which was obtained from the blood of Japanese white rabbits (male, 45 mL of blood and 5 mL of 3.8% sodium citrate aqueous solution) by centrifugation at 1000 rpm for 20 min. Samples were rinsed with saline and treated with 2.5% glutaraldehyde in saline at refrigerated temperatures overnight. The sample was rinsed with saline and dehydrated by systematic immersion in a series of ethanol−water solutions; 60, 70, 80, 90, and 100% v/v. Following critical point drying with carbon dioxide, the samples were coated with gold prior to being observed in a JEOL Hitachi S-2500 SEM or electron probe microanalyzer (EPM-810, Shimadzu) operating at an accelerating voltage of 20 kV. The medical grade segmented polyurethanes Biospan based on poly(tetramethylene oxide) (PTMO) was used as a control sample.

Materials. THF was distilled from lithium aluminum hydride to ensure dryness. DMAc was dehydrated over calcium hydride for 2 days and then vacuum distilled. Methanol was distilled in the presence of magnesium methoxide to ensure dryness, BD was commercially obtained from Nacalai Tesque, Inc., Japan, and purified by vacuum distillation. All purified solvents were dried over Molecular Sieves 4A (Wako Pure Chemical Ind. Ltd., Japan), purchased as the best commercial grade and used as received, unless otherwise noted. PBD with a number average molecular weight of M_n = 2840 and 20% of 1,2-vinyl, 60% of 1,4-trans, and 20% of 1,4-cis structure components was kindly provided by Nippon Oil and Fats, Co., Ltd. The syntheses of BDODP, BDHDP, and BDDDP have been described in detail previously.[36]

Synthesis of Phospholipid SPUs and SPUUs. The process of synthesizing phospholipid SPUs and SPUUs was similar to that reported by us recently.[31−34] The only difference was that BD or ED was used as the extender. The polymers were based on 1/2.5/0.75/0.75 molar ratio of SPU (PBD/MDI/BDXDP/BD) or SPUU (PBD/MDI/BDXDP/ED), in which the BDXDP included BDODP, BDHDP, or BDDDP. The reaction was carried out in DMAc without catalyst. The phospholipid SPUs and SPUUs were all synthesized by similar methods; therefore, a representative synthesis is shown below.

Soft Segment (PBD)

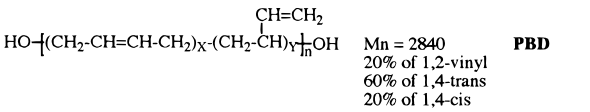

Hard Segment (MDI, BDODP, BDHDP, BDDDP, BD and ED)

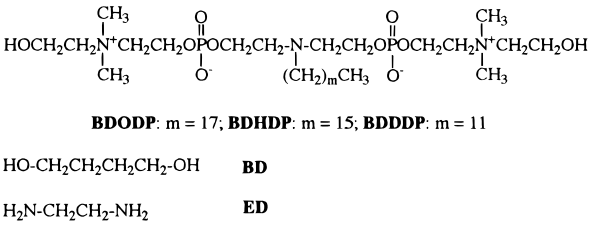

Figure 1. Chemical structures of the phospholipid SPUs and SPUUs components.

Synthesis of PBD−MDI−BDODP−BD (SPU-18). In the first step, 1.101 g (4.40 mmol) of MDI dissolved in 10 mL of DMAc was added to a stirred solution of 5.0 g (1.76 mmol) of PBD (M_n = 2840) in 10 mL of DMAc under a dry nitrogen atmosphere. After 1 h at 70−75 °C the solution was cooled to room temperature slowly. In the second step, 0.988 g (1.32 mmol) of BDODP, which was previously dissolved in 15 mL of DMAc, was slowly added into the reaction solution over 20 min. Stirring was continued at 90−95 °C for 3 h. For the last step, using the same procedure, 0.119 g (1.32 mmol) of BD, which was previously dissolved in 15 mL of DMAc, was added dropwise over another 10 min to the reaction mixture with stirring. The stirring was continued at 100 °C for 1 h. The resulting phospholipid polymer was precipitated from methanol and filtered. Following this, the polymer was washed three times with methanol. The polymer was dried in a vacuum oven at 70 °C for at least 48 h. A pale yellow elastomer of the polymer SPU-**18** (6.1 g, 85%) was obtained. IR (film): 3300 (−NH−), 2900 and 2840 (−CH_2−), 1440 (C−N stretch), 1710 (carbonyl of −NHCOO−), 1590 (aromatic C−H), 1220 (P═O), and 1060 cm^{-1} (P−O−CH_2−). Anal. Calcd for $C_{1096}H_{1611}N_{29}O_{64}P_6$: C, 80.3; H, 9.8; N, 2.5. Found: C, 79.9; H, 9.6; N, 2.9. M_w = 56 000, M_n = 30 000, polydispersity: M_w/M_n = 1.9.

The other phospholipid SPUs and SPUUs were synthesized by the procedures similar to these described above. For SPUUs, only at the last step, ED was used to instead of BD. The chemical structures of the SPUs and SPUUs components and detailed synthesis conditions for the synthesized phospholipid polymers are summarized in Figure 1 and Table 1.

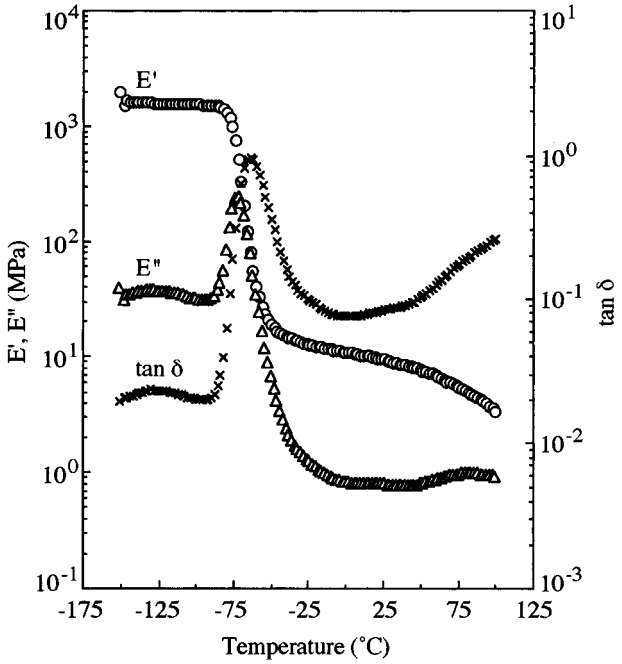

Figure 2. Temperature dependence of the storage modulus (E'), loss modulus (E''), and loss tangent (tan δ) for the phospholipid segmented polyurethane SPU-**12** at 11 Hz.

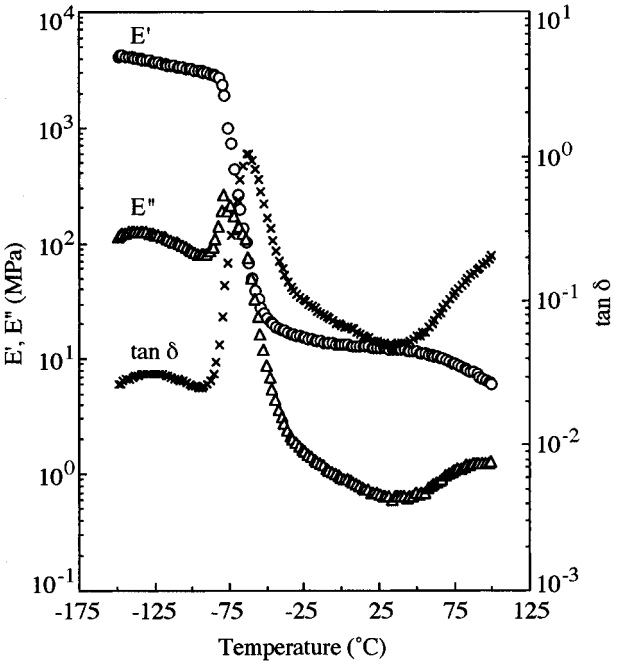

Figure 3. Temperature dependence of the storage modulus (E'), loss modulus (E''), and loss tangent (tan δ) for the phospholipid segmented poly(urethane urea) SPUU-**12** at 11 Hz.

Results and Discussion

Bulk Property Characterization. Bulk property characterization data are also summarized in Table 1. The stoichiometry of the reaction was 1:2.5:0.75:0.75 for PBD:MDI:BDXDP:BD or PBD:MDI:BDXDP:ED, respectively. BDXDP includes BDODP (for SPU-**18** and SPUU-**18**), BDHDP (for SPU-**16** and SPUU-**16**), and BDDDP (for SPU-**12** and SPUU-**12**). On the basis of monomer feed ratios, the designed hard segment was in the range 30.0−31.5%.

The molecular weights of the polymers were characterized by GPC based on polystyrene standards. From the relationship between retention time and molecular weights derived for narrow-distributed standard polystyrene, the weight average molecular weights (M_w) of SPUs-**18**, **16**, and **12** and SPUUs-**18**, **16**, and **12** were 56 000, 54 000, 59 000, 76 000, 75 000, and 72 000, respectively. Corresponding polydispersity (M_w/M_n) of SPUs-**18**, **16**, and **12** and SPUUs-**18**, **16**, and **12** was 1.9, 1.6, 1.7, 1.8, 1.5, and 1.6. These molecular weights are sufficient for most biomedical applications.

The typical results of dynamic viscoelasticity experiment for the SPU-**12** and SPUU-**12** film sample are displayed in Figures 2 and 3. For SPU-**12**, the storage modulus (E') was slowly decreased from 1.98 × 10^3 MPa at −150 °C to 1.33 × 10^3 MPa at −80 °C, following a rapid decrease with a 2-order magnifical change. The material reached the elastomer region at 15 MPa near −40 °C. The peak of tan δ at −64 °C, together with the peak of loss modules (E'') at −72 °C was observed. At 36.1 °C, 8.68 MPa, 0.763 MPa, and 0.088 for E', E'', and tan δ were observed. While for SPUU-**12** (Figure 3), the storage modulus (E') also slowly decreased from 4.15 × 10^3 MPa at −150 °C to 2.36 × 10^3 MPa at −80 °C, following a rapid decrease with 2-orders of magnificence. The material reached the elastomer region at 18 MPa near −40 °C. The peak of tan δ at −64 °C, together with the peak of loss modules (E'') at −74 °C was observed. At 36.1 °C, 12.1 MPa, 0.615 MPa, and 0.051 for E', E'', and tan δ were observed.

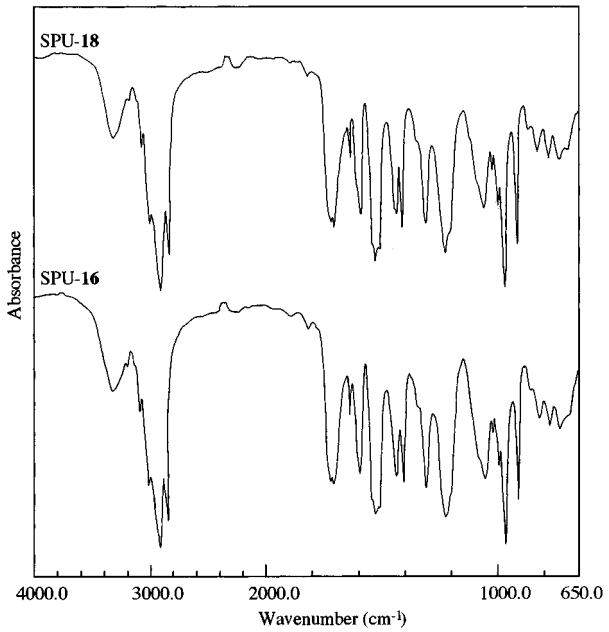

Figure 4. IR spectra of the phospholipid SPU-**18** and SPU-**16**.

Both the phospholipid segmented polyurethane SPU-**12** and poly(urethane urea) SPUU-**12** showed similar viscoelasticity profiles. They were both soft elastomers at room temperature with a softening point at near −65 °C.

The IR spectral analyses of the polymers were taken on cast films. All phospholipid polymers are related with the inclusion of PBD, MDI, and phospholipid moieties. This is clear from the complete IR spectrum of each material. Figure 4 shows the IR spectra of the typical phospholipids SPU-**18** and SPU-**16**, which shows adsorption bands due to −NH− band at 3300 cm^{-1},

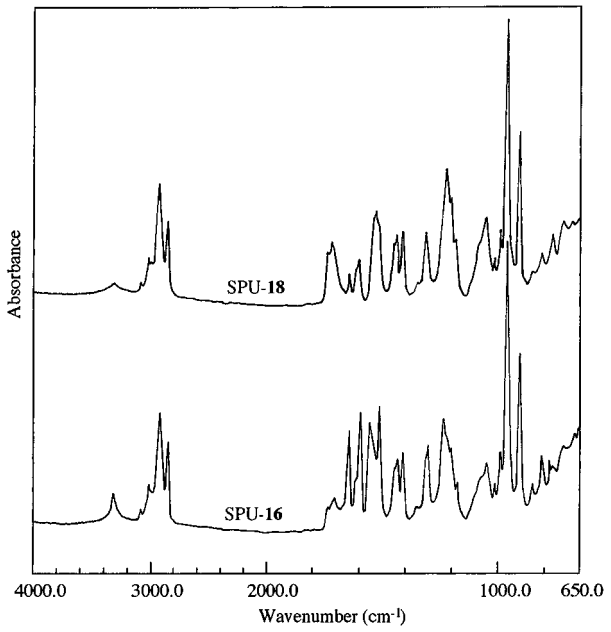

Figure 5. ATR-FTIR spectra of the phospholipid SPU-**18** and SPU-**16**.

carbonyl stretch of −NHCOO− at 1710 cm^{-1}, $-CH_2-$ band at 2900 and 2840 cm^{-1}, C−N stretching band at 1440 cm^{-1}, aromatic C−H stretches at 1590 cm^{-1}, P═O at 1220 cm^{-1}, and $P-O-CH_2-$ at 1060 cm^{-1}.

Surface Property Characterization. Surface properties of the casted films of the polymers were investigated by ATR-FTIR, ESCA, and contact angle measurements. In previous papers,[30,31,38] the surface properties and hemocompatibilities of polymers were found to be different for the surface exposed to air relative to the surface adjacent to the substrate. In this study, the air-facing surface of the phospholipid polymers was the blood contacting surface; therefore, all surface and hemocompatible properties were related to air facing surface.

Figure 5 shows the ATR-FTIR spectra of the typical phospholipids SPU-**18** and SPU-**16**. The spectra of the polymers give evidence of unsaturated C═C bonds, PO_4^-, N−H, C═O, quaternary ammonium, nonbonded and bonded urethane, and unsaturated aromatic bonds. The analysis of PBD composition has been discussed in detail in our previous article.[31] The peaks at 3075 cm^{-1} are CH═CH unsaturated vinyl stretches, at 964 cm^{-1} are the trans 1,4-addition of CH═CH, at 680 cm^{-1} are the cis 1,4-addition of CH═CH, and at 993 and 910 cm^{-1} are 1,2-addition of $CH=CH_2$ stretches. The N−H absorption band was observed at 3311 cm^{-1}. The peak at 1708 cm^{-1} has been assigned to carbonyl groups that are hydrogen bonded (presumably to the urethane hydrogens) and the peak at 1724 cm^{-1} has been assigned to carbonyl groups that are not hydrogen-bonded. Moreover, the relatively weaker band at 1641 cm^{-1} owing to the amide I stretch, the peak at 1595 cm^{-1} due to aromatic C−H stretching, and the important frequency at 1221 cm^{-1} due to P═O bond of phospholipid stretching were clearly observed.

No important difference between the bulk IR and surface ATR-FTIR spectra for the typical phospholipids SPU-**18** and SPU-**16** was observed, merely that the intensity of N−H band and carbonyl groups showed relatively weaker absorption in the ATR−FTIR spectra.

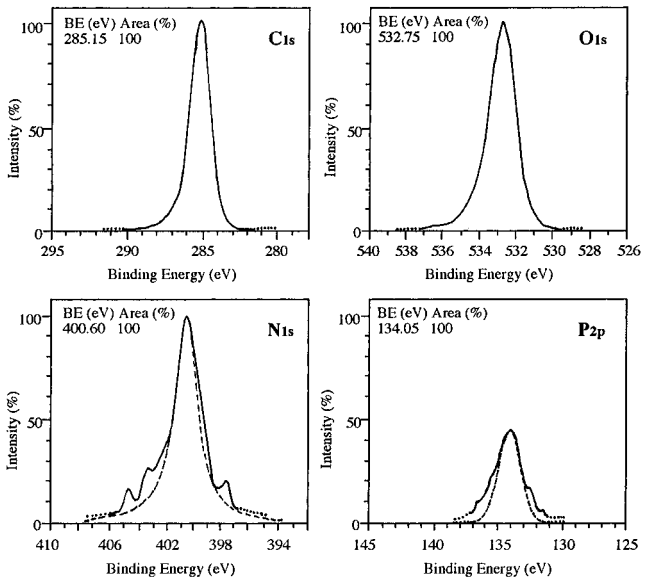

Figure 6. ESCA spectra of the cast film surface of phospholipid SPU-**16**.

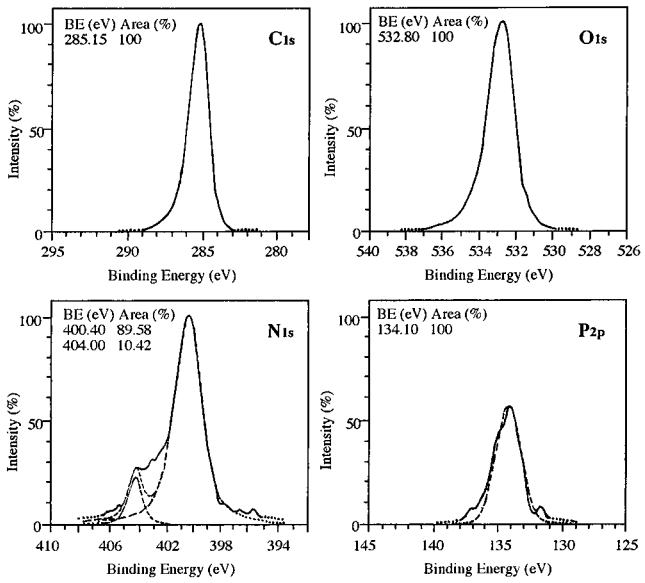

Figure 7. ESCA spectra of the cast film surface of phospholipid SPUU-**16**.

Figures 6 and 7 show typical C_{1s}, O_{1s}, N_{1s}, and P_{2p} ESCA spectra for SPU-**16** and SPUU-**16** acquired at a 60° takeoff angle. C_{1s}, O_{1s}, N_{1s}, and P_{2p} envelopes for SPU-**16**, shown in Figure 6, suggest a surface dominated by the PBD soft segment with urethane. The urethane (NH−**C**OO) peak compared to the hydrocarbon (C−**C**−C) peak at 285.15 eV are too small to allow accurate peak resolution. A Gaussian peak at 532.75 eV was used to fit the SPU-**16** O_{1s} peak. The high-energy and low-energy tailings on the O_{1s} peak reflect a combination of hole-state lifetime broadening contributions from the urethane oxygens (N−CO**O** and N−C**O**O) and phosphorus oxygens ($P\mathbf{O}_4^-$). The high-energy and low-energy tailings on the N_{1s} peak also reflect a combination of hole-state lifetime broadening contributions from the urethane nitrogen (**N**−COO), phospholipid ammonium nitrogen ($-\mathbf{N}^+(CH_3)_2-$), and amine nitrogen (>**N**−

(38) Paik Sung, C. S.; Hu, C. B. *J. Biomed. Mater. Res.* **1979**, *13*, 161.

Table 2. ESCA Elemental Surface Composition (%) of the Phospholipid SPUs and SPUUs[a]

polymers	C_{1s}	O_{1s}	N_{1s}	P_{2p}	O_{1s}/C_{1s}	N_{1s}/C_{1s}	P_{2p}/C_{1s}
SPU-**18**	80.83(80.31)	17.49(6.25)	1.39(2.48)	0.29(1.14)	0.2164	0.0172	0.0036
SPU-**16**	82.62(80.28)	15.28(6.28)	1.68(2.49)	0.42(1.14)	0.1850	0.0203	0.0051
SPU-**12**	83.34(80.23)	14.49(6.35)	1.74(2.52)	0.43(1.15)	0.1738	0.0209	0.0051
SPUU-**18**	84.27(80.31)	14.59(5.70)	0.93(3.01)	0.20(1.14)	0.1732	0.0111	0.0024
SPUU-**16**	81.92(80.28)	15.65(5.73)	1.88(3.02)	0.56(1.15)	0.1911	0.0229	0.0068
SPUU-**12**	82.20(80.23)	15.67(5.79)	1.77(3.06)	0.36(1.16)	0.1906	0.0215	0.0044

[a] Values in parentheses are expected theoretical elemental bulk composition (%).

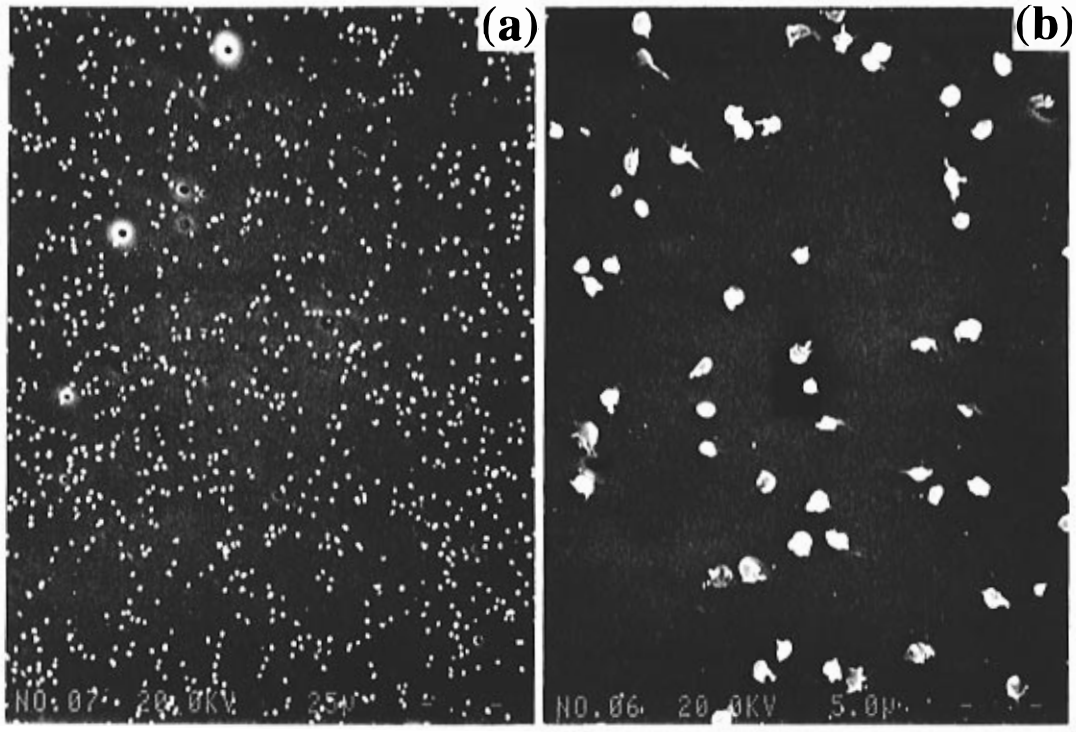

Figure 8. SEM photographs of the surface of medical grade BioSpan films cast from DMAc solution after 60 min of rabbit PRP exposure. Actual magnification: (a) ×400; (b) ×2000.

$(CH_2)_mCH_3$). The nitrogen binding energy was at 400.60 eV. A Gaussian peak at 134.05 eV was used to fit the P_{2p} peak ($\mathbf{P}O_4^-$).

Details from the ESCA spectra for SPUU-**16** are shown in Figure 7. Compared to the results in Figure 6, there was no significant difference between the SPU-**16** and SPUU-**16** except that the N_{1s} peak can be resolved into two peaks. A 89.58% Gaussian peak at 400.40 eV for the urethane nitrogen (**N**−COO), phospholipid ammonium nitrogen ($-\mathbf{N}^+(CH_3)_2-$), and amine nitrogen ($>\mathbf{N}-(CH_2)_mCH_3$) and 10.42% Gaussian peak at 404.00 eV for the urea nitrogen (**N**−CO−**N**) were used to fit the SPUU-**16** N_{1s} peak. Another minor difference was the binding energy and their relative composition ratio based on area. The C_{1s} spectrum for SPUU-**16** also suggest a surface dominated by the PBD soft segment with urethane and urethane urea. The urethane (NH−**C**OO) and urea (N−**C**O−N) peaks compared to the hydrocarbon (C−**C**−C) peak at 285.15 eV are too small to allow accurate peak resolution. A Gaussian peak at 532.80 eV was used to fit the SPUU-**16** O_{1s} peak. The high-energy and low-energy tailings on the O_{1s} peak reflect a combination of hole-state lifetime broadening contributions from the urethane oxygens (N−CO**O** and N−C**O**O), urea oxygens (N−C**O**−N) and phosphorus oxygens ($P\mathbf{O}_4^-$). A Gaussian peak at 134.10 eV was used to fit the P_{2p} peak ($\mathbf{P}O_4^-$).

Table 2 lists ESCA elemental surface compositions of the synthesized polymers. All samples show the most amount of C_{1s} and the less P_{2p} on the surface of the polymers. Comparing the elemental bulk and surface compositions, it is found that almost all carbon composition was arranged on the surface of the cast films. Excess oxygen composition on the surface may be owing to the absorbed water in the air; this result suggests that incorporating the phospholipids directly into the polymer backbone may make the materials be able to keep some water content in the materials. This is important for biomaterials because the biomaterials should "work" in water. Moreover, 25.4, 36.8, 37.4, 17.5, 48.7, and 31.0% phosphorus content arranged on the surface of the SPU-**18**, SPU-**16**, SPU-**12**, SPUU-**18**, SPUU-**16**, and SPUU-**12** cast films were also observed. The ratio of the peak area of oxygen, nitrogen, and phosphorus to that of carbon (O_{1s}/C_{1s}, N_{1s}/C_{1s}, and P_{2p}/C_{1s}) was calculated and also summarized in Table 2. The P_{2p}/C_{1s} value of the samples was in the range 0.0024−0.0068.

To investigate the hydrophilicity−hydrophobicity of the surface of the polymers, water contact angle measurements were carried out (Table 3). As expected, the relatively big contact angles indicated that these polymers had hydrophobic surfaces. SPUs-**18**, **16**, and **12** exhibited contact angle of 94.5 ± 2°, 92.2 ± 4°, and 90.9

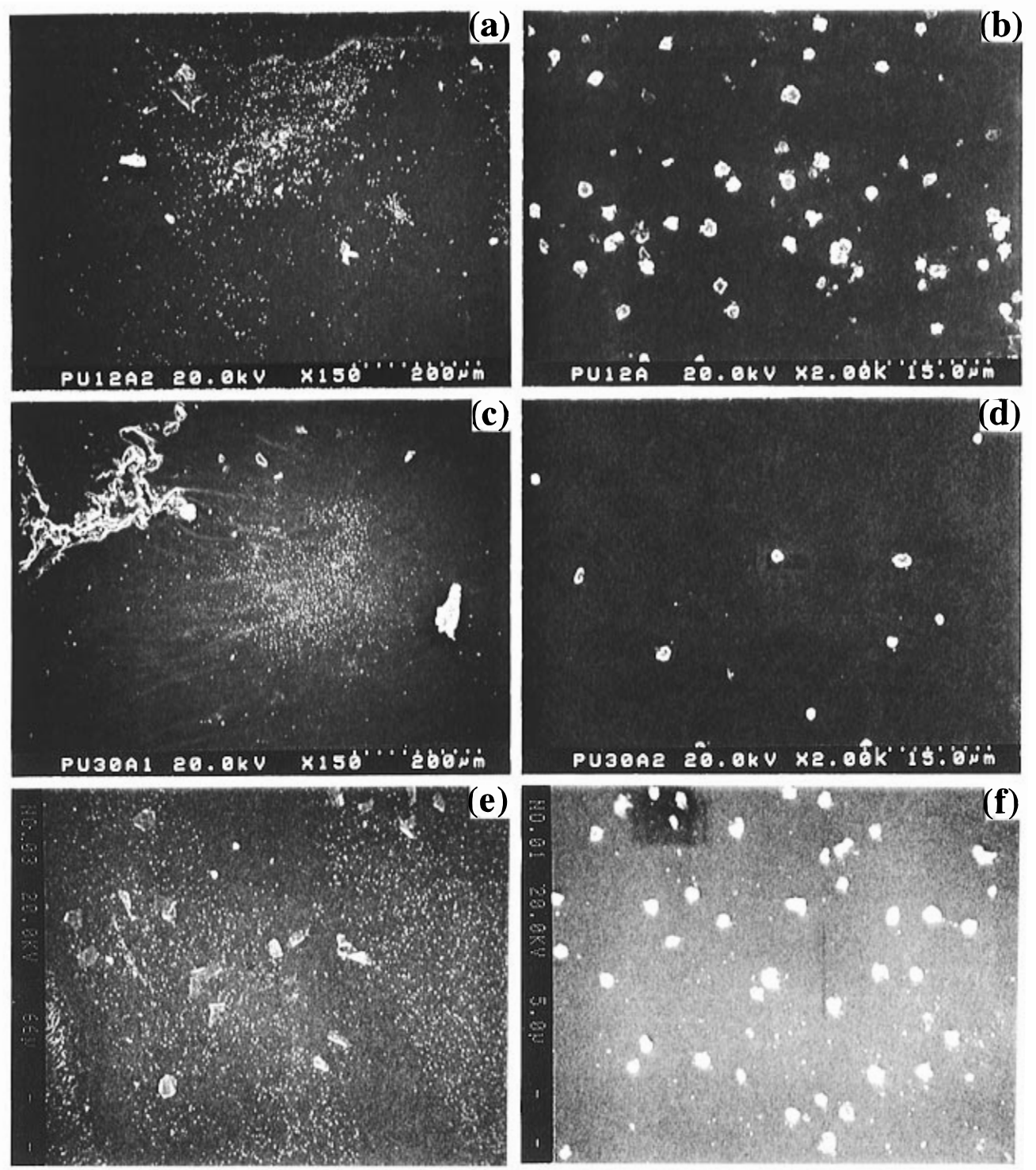

Figure 9. SEM photographs of the surface of phospholipid SPUs films cast from mixed DMAc and THF (volume ratio 1/1) solution after 60 min of PRP exposure. (a and b) SPU-**18**; (c and d) SPU-**16**; (e and f) SPU-**12**. Actual magnification: (a, c, and e) ×150; (b, d, and f) ×2000.

Table 3. Water Contact Angle of the Phospholipid SPUs and SPUUs

polymers	chemical compositions	water contact angle (deg)
SPU-**18**	PBD−MDI−BDODP−BD	94.5 ± 2
SPU-**16**	PBD−MDI−BDHDP−BD	92.2 ± 4
SPU-**12**	PBD−MDI−BDDDP−BD	90.9 ± 2
SPUU-**18**	PBD−MDI−BDODP−ED	93.7 ± 2
SPUU-**16**	PBD−MDI−BDHDP−ED	91.6 ± 4
SPUU-**12**	PBD−MDI−BDDDP−ED	90.7 ± 2

± 2°. SPUUs-**18**, **16**, and **12** exhibited contact angle of 93.7 ± 2°, 91.6 ± 4°, and 90.7 ± 2°. This result agrees with that of ESCA: samples with highest carbon content (and largest alkyl chains) are the most hydrophobic.

Hemocompatibility Evaluation. The synthesized SPUs and SPUUs were assessed as biomaterials mainly by the degree and nature of blood platelet adhesion resulting from exposure to platelet-rich plasma (PRP) for 60 min. The specimens incubated in PRP were viewed by SEM. The typical SEM photographs of medical grade BioSpan, SPUs-**18**, **16**, and **12**, and SPUUs-**18**, **16**, and **12** are shown in Figures 8−10.

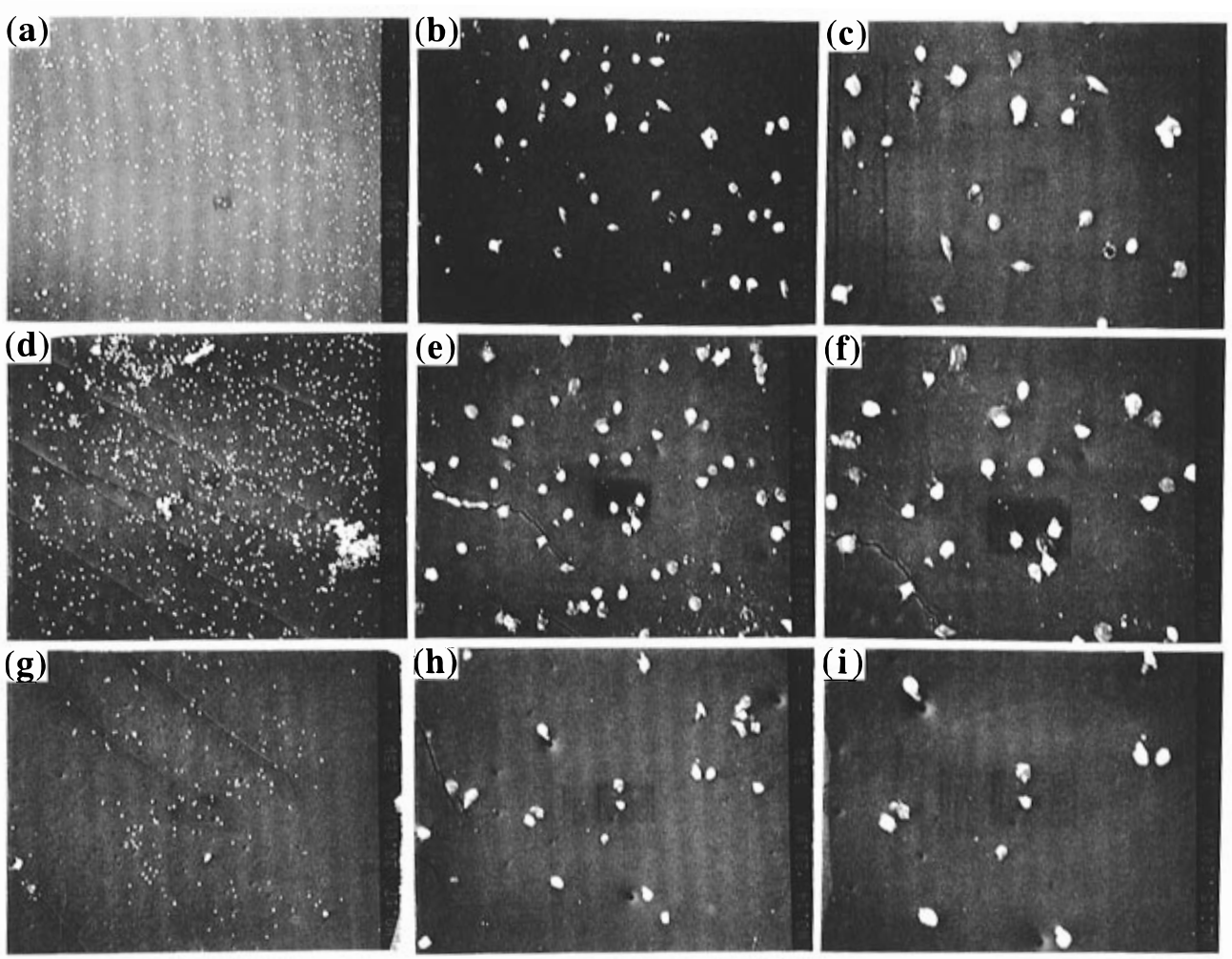

Figure 10. SEM photographs of the surface of phospholipid SPUUs films cast from mixed DMAc and THF (volume ratio 1/1) solution after 60 min of PRP exposure. (a, b, and c) SPUU-**18**; (d, e, and f) SPUU-**16**; (g, h, and i) SPUU-**12**. Actual magnification: (a, d, and g) ×400; (b, e, and h) ×2000; (c, f, and i) ×3000.

For medical grade segmented polyurethane BioSpan, a substantial number of platelets adhered and were finning to elongated (Figure 8). However, for synthesized phospholipid SPUs and SPUUs, especially for SPU-**16** and SPUU-**12**, a relatively limited number of platelets adhered and the cells remained rounded with no extensions formed. Generally, it seemed that the apparent degree of changing shape of platelets was in the order: BioSpan > SPUUs > SPUs. Among the SPUUs-**18**, **16**, and **12** or among the SPUs-**18**, **16**, and **12**, there was not a significant difference on the adhered platelet variation. On the basis of the SEM observation, the number of adhered platelets in an area of 10 μm × 10 μm was 2.3, 2.1, 1.7, 1.5, 1.4, 0.8, and 0.4 for BioSpan, SPUU-**16**, SPU-**12**, SPUU-**18**, SPU-**18**, SPUU-**12**, and SPU-**16**, respectively.

These results indicated that the hemocompatibility of the synthesized phospholipid polymers was generally better than that of medical grade segmented polyurethanes BioSpan. SPU-**16** and SPUU-**12** were the best hemocompatible materials among all samples. This result indicated that suitable alkyl chain length in the polymer side chain may be a useful factor to adjust the amphiphilic properties of the polymer surface and to affect the hemocompatibilities of the materials.

Acknowledgment. We are grateful to Nippon Oil and Fats, Co., Ltd., and Polymer Technology Group Incorporated of USA, for kindly providing the poly(butadiene) glycol and BioSpan sample.

CM960615O